J. Phys. Chem. A **1999,** *103,* 1025−1028

Vanadium and Niobium Hexadinitrogen and Hexacarbonyl Complexes: Electron-Spin-Resonance Spectra at 4 K

S. H. Parrish, R. J. Van Zee, and W. Weltner, Jr.*

Department of Chemistry, University of Florida, Gainesville, Florida 32611-7200

Received: October 5, 1998

Electron-spin-resonance (ESR) spectroscopy has been applied to vanadium, niobium (and tantalum) complexes with N_2 and CO in the corresponding pure solid matrixes at 4 K. Except for $V(CO)_6$, none has previously been studied by ESR. For these d,[5] $S = {}^1/_2$, radicals, g values and hyperfine parameters (^{51}V, ^{93}Nb nuclei) are obtained and interpreted in terms of axial molecules, distorted from octahedral symmetry by Jahn−Teller effects. There are significant differences with previous work, and the new metal hyperfine data in the two types of complexes are informative.

Introduction

The objective of this research is to observe the hexadinitrogen complexes of vanadium, niobium, and tantalum via electron-spin-resonance (ESR) spectroscopy. None of these molecules has been studied previously by ESR. Each hexacomplex is formed by trapping the metal atoms in either pure solid N_2 or CO. The interest here is in a more intimate experimental comparison of N_2 and CO as ligands in transition-metal complexes. The ligand ← metal σ donation and metal → ligand π acceptance applies to both CO and N_2, but apparently N_2 is a poorer σ donor than is CO and its bonding is weaker.[1,2]

There is a large body of literature on transition-metal carbonyls, and that interest, particularly along theoretical lines, continues to this day.[3,4] $V(CO)_6$ has been studied in a variety of experiments,[5−14] including ESR,[11−14] but the results are not consistent. Electronic spectra of $V(N_2)_6$ and $V(CO)_6$ have been compared and discussed via crystal-field and charge-transfer effects.[15,16] Our ESR studies here of the hexa-carbonyls of niobium and tantalum are also new; although $Ta(CO)_6$ has been observed earlier in the optical and infrared regions,[17] and some dinitrogen complexes of Nb have been observed in the infrared.[18]

All of these molecules are expected to be basically octahedral with the unpaired electron in the lower degenerate T_{2g} orbital so that the molecules are susceptible to Jahn−Teller distortion. The distortion can often not be established as forming a trigonal or a tetragonal symmetry axis, but for $V(CO)_6$ the latter is favored with a $^2B_{2g}$ ground state.[10−13] One therefore expects that picture to prevail among the Nb and Ta hexacarbonyls and also among their hexadinitrogen complexes.

A definitive axial ESR spectrum of $Nb(CO)_6$ is obtained here, but the $Ta(CO)_6$ spectrum is broad and difficultly assigned.. The dinitrogen complexes of V and Nb yield unique spectra involving overlap of perpendicular and parallel lines, but the analyses yield parameters in accord with expectations when the CO ligand is replaced by N_2.

Experimental Section

Vanadium rod [99.9% purity, 99.75% ^{51}V ($I = {}^7/_2$), 0.25% $^{50}V(I = 6)$] and niobium rod [99.8% purity, 100% ^{93}Nb ($I = 9/2$)] were purchased from Aesar. Tantalum rod [99.5% purity, 99.99% ^{181}Ta ($I = {}^7/_2$), 0.01% ^{180}Ta ($I = 0$)] was purchased from Fansteel. All of these rods are 6.35 mm diameter and were rotated in the laser beam during vaporization.

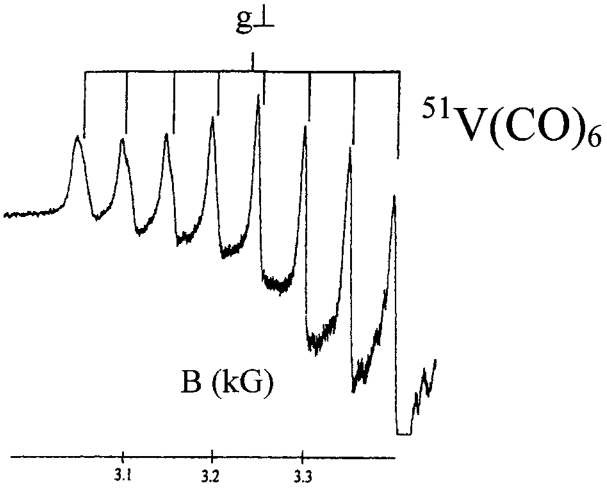

Figure 1. ESR spectrum of $^{51}V(CO)_6$ in solid CO at 2 K ($\nu = 9.5228$ GHz). The parallel lines form a broad band centered at 3430 G.

Carbon monoxide (99.99% purity) and nitrogen (99.999% purity) were purchased from Airco and used directly. The spectrometer, Heli-Tran, and laser have been previously described.[19]

Concentrations of the carbonyl and dinitrogen complexes in these matrixes were probably less than 1%; the laser power was varied to obtain the optimum spectra.

Results

X-band (9.5 GHz) ESR spectra of $^{51}V(CO)_6$ and $^{93}Nb(CO)$ in solid CO and of $^{51}V(N_2)_6$ and $^{93}Nb(N_2)_6$ in solid N_2 at 4 K are shown in Figures 1−4. Line widths are of the order of 10 G. Corresponding spectra of $^{181}Ta(CO)_6$ and $^{181}Ta(N_2)_6$ were observed but were very broad and not amenable to analysis. We feel that the tantalum spectra are severely affected by the large quadrupole interaction with that nucleus, making the normally forbidden $\Delta M_I = \pm 2$ transitions appear strongly. Lines which could be interpreted as hyperfine structure are irregularly spaced and difficult to assign.

For $V(CO)_6$ only the distinctive ^{51}V hyperfine splittings (hfs) ($I = 7/2$) centered around 3.2 kG are shown in Figure 1. The

10.1021/jp983952o CCC: $18.00

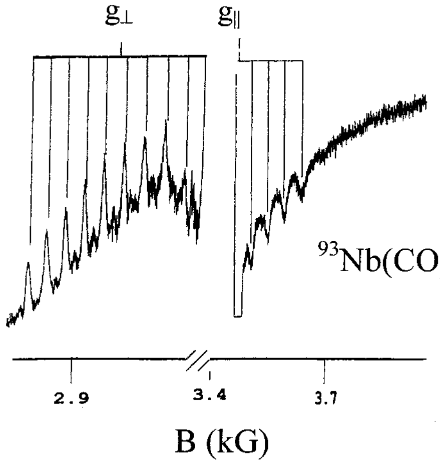

Figure 2. ESR spectrum ^{93}Nb(CO)$_6$ in solid CO at 2 K ($\nu = 9.5241$ GHz). The gain on the parallel lines is twice that of the perpendicular lines.

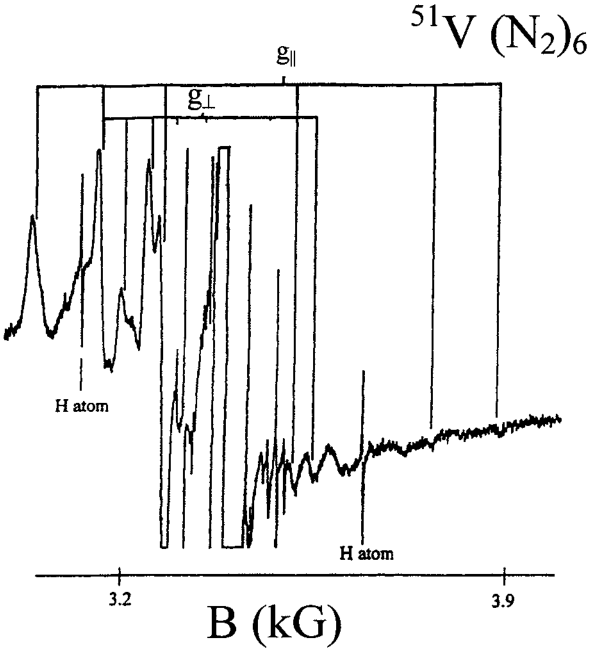

Figure 3. ESR spectrum of ^{51}V(N$_2$)$_6$ in solid N$_2$ at 4 K ($\nu = 9.5367$ GHz).

parallel lines, with small undetectable hf, produce a broad line of opposite phase at high field (at $g_{\parallel} \cong 1.98$) as previously observed by Rubinson[12] and by Bratt et al.[13] in frozen glasses. Our carbonyl spectra are those of axial molecules. That shows up very clearly in the Nb(CO)$_6$ spectrum in Figure 2 where the perpendicular hf lines ($I = {}^9/_2$) occur at low magnetic fields and the parallel lines, of opposite phase, at higher fields. Nonaxiality would be evident if the perpendicular lines showed shoulders or splittings requiring a third g value to be included in the analysis. The observed spectra in Figures 1 and 2 require any such distortions to be within the line widths and therefore very small.

The dinitrogen spectra, in pure solid nitrogen at 4 K, shown in Figures 3 and 4 are distinctly different from these carbonyl spectra. The major cause of this is an increase of the metal hfs in the parallel lines ($|A_{\parallel}|$) when N$_2$ replaces CO. These changes produce strong overlap of parallel and perpendicular features leading to phase variations which cause the analyses to be more difficult and uncertain. No ^{14}N hfs was observed.

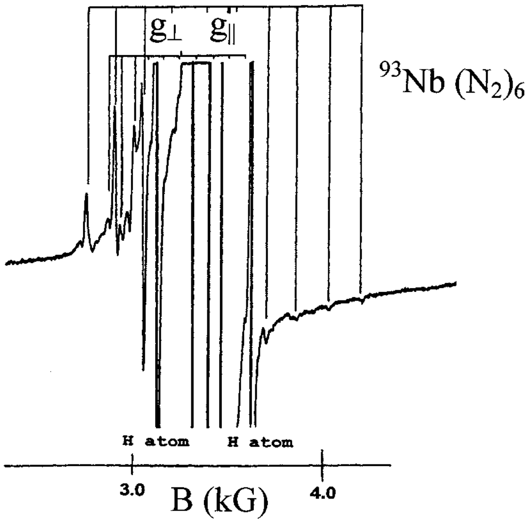

Figure 4. ESR spectrum of ^{93}Nb(N$_2$)$_6$ in solid N$_2$ at 4 K ($\nu = 9.5341$ GHz).

TABLE 1: Observed and Calculated[a] Line Positions for ^{51}V(CO)$_6$ in Solid CO at 4 K ($\nu = 9.5228$ GHz)

M_I (^{51}V)	observed ⊥ (G)	calcd ⊥ (G)	observed ∥ (G)
$^7/_2$	3051(5)	3052.0	
$^5/_2$	3098	3099.5	
$^3/_2$	3147	3147.5	
$^1/_2$	3198	3195.8	broad line at 3430 G
$-^1/_2$	3247	3244.5	
$-^3/_2$	3298	3293.6	
$-^5/_2$	3348	3348.2	
$-^7/_2$	3398	3392.9	

[a] Calculated using $g_{\perp} = 2.111$, $A_{\parallel}(^{51}\mathrm{V}) = -21$ MHz, $A_{\perp}(^{51}\mathrm{V}) = +143.8$ MHz (see Table 5).

Analysis

The observed lines were fit using an axial S = $^1/_2$ Hamiltonian[20]

$$H = g_{\parallel}\beta B_z S_z + g_{\perp}\beta(B_x S_x + B_y S_y) + A_{\parallel} S_z I_z + A_{\perp}(S_x I_x + S_y I_y) \quad (1)$$

where $I = {}^7/_2$ for ^{51}V and $^9/_2$ for ^{93}Nb. The results of the computer-aided exact fits are shown in Tables 1−4 for ^{51}V(CO)$_6$, ^{93}Nb(CO)$_6$, ^{51}V(N$_2$)$_6$, and ^{93}Nb(N$_2$)$_6$, respectively. The relative signs of the hyperfine components are not determined, but in order to obtain a reasonable d-electron spin density for ^{93}Nb(CO)$_6$, and probably also for ^{51}V(CO)$_6$, $A_{\parallel}$ and $A_{\perp}$ were taken to have opposite signs. For ^{51}V(N$_2$)$_6$ and ^{93}Nb(N$_2$)$_6$ this was not necessary and in fact doing so gave a totally unreasonable dipolar hf parameter A_{dip}. $g_{\parallel} = 1.98$ of V(CO)$_6$ was taken at the peak of the broad feature at 3430 G (not shown in Figure 1).

Derived magnetic parameters for the vanadium and niobium complexes are collected in Table 5.

Discussion

Tetragonal axial elongation (Jahn−Teller effect) of the octahedral crystal field leads to D_{4h} symmetry, with the energy-level scheme shown in Figure 5. The unpaired d$_{xy}$ electron then yields a ^{2}B$_{2g}$ ground state. The ESR spectra measured here indicate that such an axial molecule is correct, and we assume that both the carbonyls and dinitrogen complexes follow this scheme.

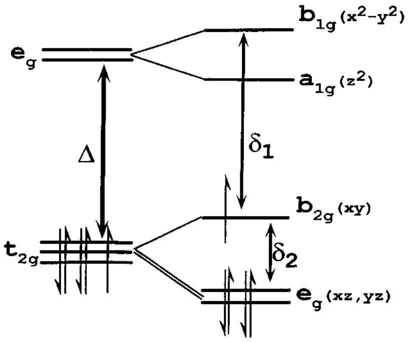

Figure 5. Molecular orbital diagram showing the origin of the octahedral (Δ) and Jahn−Teller energies for tetragonal distortion. In general $\Delta \cong \delta_1 \gg \delta_2$.

TABLE 2: Observed and Calculated[a] Line Positions for ^{93}Nb(CO)$_6$ in Solid CO at 4 K (ν = 9.5241 GHz)

M_I (^{93}Nb)	observed ⊥ (G)	calcd ⊥ (G)	observed ∥ (G)	calcd ∥ (G)
$^9/_2$	2782(5)	2782.9		3288.7
$^7/_2$	2842	2841.5		3323.4
$^5/_2$	2899	2900.9		3359.5
$^3/_2$	2961	2961.2		3397.0
$^1/_2$	3021	3022.4		3436.0
$-1/_2$	3085	3084.3		3476.3
$-3/_2$	3147	3147.1	3515(5)	3518.2
$-5/_2$	3214	3210.8	3559	3561.4
$-7/_2$	3275	3275.3	3605	3606.0
$-^9/_2$		3340.5	3650	3652.1

[a] Calculated using $g_{\parallel}$ = 1.959, $g_{\perp}$ = 2.2212, $A_{\parallel}$(^{93}Nb) = −111 MHz, $A_{\perp}$(^{93}Nb) = +193 MHz (see Table 5).

TABLE 3: Observed and Calculated[a] Lines for ^{51}V(N$_2$)$_6$ in Solid N$_2$ at 4 K (ν = 9.5367 GHz)

M_I (^{51}V)	observed ⊥ (G)	calcd ⊥ (G)	observed ∥ (G)	calcd ∥ (G)
$^7/_2$	3160	3155.1	3044(5)	3042.2
$^5/_2$	3208(5)	3202.8	3160	3160.9
$^3/_2$	3253	3253.1	3276	3279.6
$^1/_2$		3306.0		3399.2
$-^1/_2$		3361.4	3521	3519.7
$-^3/_2$		3419.2		3641.2
$-^5/_2$		3479.4	3763	3763.5
$-^7/_2$	3541	3541.9	3889	3886.9

[a] Calculated using $g_{\parallel}$ = 1.965, $g_{\perp}$ = 2.032, $A_{\parallel}$(^{51}V) = +332 MHz, $A_{\perp}$(^{51}V) = +153 MHz (See Table 5).

TABLE 4: Observed and Calculated[a] Line Positions for ^{93}Nb(N$_2$)$_6$ in Solid N$_2$ at 4 K (ν = 9.5341 GHz)

M_I (^{93}Nb)	observed ⊥ (G)	calcd ⊥ (G)	observed ∥ (G)	calcd ∥ (G)
$^9/_2$	2871(3)	2873.9	2751(5)	2749.6
$^7/_2$	2936	2936.0	2902	2904.9
$^5/_2$	3003	3003.4	3055	3062.2
$^3/_2$		3075.6	3216	3221.8
$^1/_2$		3152.7		3383.6
$-^1/_2$		3234.4	3545	3547.6
$-^3/_2$		3320.7	3718	3713.7
$-^5/_2$		3411.4	3882	3882.1
$-^7/_2$	3503	3506.5	4054	4052.6
$-^9/_2$	3602	3605.8	4227	4225.4

[a] Calculated using $g_{\parallel}$ = 1.9505, $g_{\perp}$ = 2.0958, $A_{\parallel}$(^{93}Nb) = +448 MHz, $A_{\perp}$(^{93}Nb) = +238 MHz (see Table 5).

TABLE 5: Derived Magnetic Parameters of Vanadium and Niobium Hexacarbonyls and Hexadinitrogen Complexes

	^{51}V(CO)$_6$	^{93}Nb(CO)$_6$	^{51}V(N$_2$)$_6$	^{93}Nb(N$_2$)$_6$
$g_{\parallel}$	1.98(2)	1.959(1)	1.965(1)	1.9505(5)
$g_{\perp}$	2.111(1)	2.2212(5)	2.032(1)	2.0958(9)
$\lvert A_{\parallel}\rvert$ (MHz)	21(3)[a,b]	111(3)[a]	332(1)	448(1)
$\lvert A_{\perp}\rvert$ (MHz)	143.8(6)[a]	193(1)[a]	153(3)	238(2)
$\lvert A_{\mathrm{iso}}\rvert$ (MHz)	89(1)[a]	92(2)[a]	213(2)	308(2)
$\lvert A_{\mathrm{dip}}\rvert$ (MHz)	55(1)[a]	101(1)[a]	58(1)	70(1)

[a] $A_{\parallel}$ and $A_{\perp}$ are taken as having opposite signs. [b] $A_{\parallel}$ estimated from line width and second-order effects.

TABLE 6: Crystal-Field and Jahn−Teller Parameters for Hexacarbonyl and Hexadinitrogen Complexes of Vanadium and Niobium

	k[a]	δ_1 (cm^{-1})[b]	δ_2 (cm^{-1})[b]
V(CO)$_6$	0.44	7000[c,d]	330[c,d,e]
V(N$_2$)$_6$	0.46	4500[f]	1400
Nb(CO)$_6$	0.77	40000	2000
Nb(N$_2$)$_6$	0.53	16000	2300[g]

[a] Derived from Table 5 and A_{dip} (complex)/A$_{\mathrm{dip}}$ (metal atom). See text. [b] See Figure 5. [c] 36200 and 1880 cm^{-1} for δ_1 and δ_2 from ref 11. [d] 25840 and 4640 cm^{-1} from ref 16. [e] 1350 cm^{-1} from ref 12. [f] 19 455 cm^{-1} from ref 16. [g] 4130 cm^{-1} from ref 16.

Then the only state symmetry that can couple with the ground state to produce the observed $g_{\parallel}$ is B$_{1g}$. L$_z$ transforms as A$_{2g}$ in D_{4h} and the only nonzero integral is thus $\langle B_{1g}|A_{2g}|B_{2g}\rangle$. L$_{x,y}$ transform as E$_g$ and the only state coupling to produce $g_{\perp}$ is E$_g$ ($\langle E_g|E_g|B_{2g}\rangle$). B$_{1g}$ is an "electron" state and E$_g$ a "hole" state so that $g_{\parallel}$ is less than g_e and $g_{\perp}$ is greater than g_e, as observed. It is seen that δ_1(B$_{1g}$ − B$_{2g}$) is roughly Δ, and δ_2 (E$_g$ − B$_{2g}$) is the Jahn−Teller distortion energy.

The theory accounting for $g_{\parallel}$ and $g_{\perp}$ shifts for an octahedral d^5 complex in the "low-spin" state undergoing Jahn−Teller tetragonal elongation has been developed by Stevens[21] and others.[22] For D_{4h} symmetry the g shifts are

$$\Delta g_{\parallel} = g_e \rightarrow 8\lambda k^2/\delta_1 \qquad (2A)$$

where δ_1 and δ_2 are as indicated in Figure 5. λ is the one-

$$\Delta g_{\perp} = g_e + 2\lambda k^2/\delta_2 \qquad (2B)$$

electron spin−orbit coupling constant, taken as λ(V) = 95 cm^{-1} and λ(Nb) = 365 cm^{-1}.[23] k is the orbital reduction factor, which is a measure of covalency, i.e., deviations from atomic orbitals. Here it has been taken as A_{dip}(complex)/A$_{\mathrm{dip}}$(metal atom).[13] For the atoms, $A_{\mathrm{dip}}(d\delta) = -\,^2/_7$P, where P is defined as in Morton and Preston,[24,20] so that A$_{\mathrm{dip}}$ (atom) = 125 MHz for ^{51}V and 131 MHz for ^{93}Nb. These k values must be considered as very uncertain, but at least they are obtained on a consistent basis. Then the substitution of the experimental data from Table 5 into eqs 2 yields the values of k, δ_1, and δ_2 given in Table 6.

In general the values of δ in Table 6 for V(CO)$_6$ depart considerably from those derived from other ESR[11−14] studies (see the footnotes to Table 6). However, Pratt and Myers'[11] values are in complete agreement with these if one includes k (0.44) in their equations. Bratt et al.[13] interpret their ESR spectra as that of a nonaxial molecule and therefore reject D_{4h} for D_{2h} symmetry. Rubinson[12] interprets his ESR spectra in terms of only one δ value which is found to be 1327 cm^{-1}. The deduced g values in n-pentane generally agree with those found here. The ESR measurements of Ammeter et al.[14] are made on V(CO)$_6$ diluted in diamagnetic host crystals such as Cr(CO)$_6$ and yield orthorhombic g tensors corresponding to neither pure tetragonal or pure trigonal distortions; therefore, we do not consider them for comparison here. The only other δ data for the two dinitrogen complexes are from optical studies[15,16] and are less definitive. These authors use the ESR estimates of Pratt and Myers[11] to assign d → d transitions.

From Table 6, it is seen that δ_1 (or Δ) is larger for the carbonyl molecules than the dinitrogen molecules, as expected for the stronger CO ligand. It is also clear that the increased spin−orbit effect in the heavier metal produces a large increase in δ_1. On the other hand, δ_2 is larger in the dinitrogen complexes than in the carbonyls.

The metal hyperfine splitting information is especially interesting. The hfs parameters in Table 5 show that $|A_\perp|$ is roughly the same when comparing CO and N_2 complexes of a particular metal. However, $A_\parallel$ increases from a small negative value in the hexa-carbonyl to a large positive value in the hexadinitrogen complexes. One then deduces [from $A_{iso} = (A_\parallel + 2A_\perp)/3$] that the corresponding isotropic hfs parameters $|A_{iso}|$ are greatly increased in the N_2 complexes, implying a larger s-character contribution to the unpaired-electron orbital. One calculates from the approximate procedure of comparison with the free-atom values of A_{iso},[24,20] that the s contribution increases from about 2% to 5% from the CO to N_2 complexes for both V and Nb. The reason for this is probably the lowering of the A_{1g} orbital to provide increased σ mixing in the unpaired-electron orbital. The s−d_{z2} (or s−pσ−dσ) hybridization of the axial metal orbital in N_2 complexes implies increased extension, which appears to be in accord with increasing δ_2 from CO to N_2 complexes.

References and Notes

(1) Cotton, F. A.; Wilkinson, G. *Advanced Inorganic Chemistry*; Interscience: NY, 1972; pp 555−567, 590−593.

(2) Chatt, J.; Melville, D. P.; Richards, R. L. *J. Chem. Soc. A* **1969**, 2841.

(3) Jones, V.; Thiel, W. *J. Chem. Phys.* **1995,** *102*, 8474−8484.

(4) Jones, V.; Thiel, W. *Organometallics* **1998**, *17*, 353−360.

(5) Haas, H.; Sheline, R. K. *J. Am. Chem. Soc.* **1966**, *88*, 3219−3220.

(6) Keller, H. J.; Laubereau, P.; Nothe, D. *Z. Naturforsch. B* **1969**, *24*, 257−258.

(7) Evans, S.; Green, J. C.; Orchard, A. F.; Saito, T.; Turner, D. W. *Chem. Phys. Lett.* **1969**, *4*, 361−362.

(8) Bellard, S.; Rubinson, K. A.; Sheldrick, G. M. *Acta Crystallogr. Sect. B* **1979**, *B35*, 271−274.

(9) Schmidling, D. G. *J. Mol. Struct.* **1975**, *24*, 1−8.

(10) Barton, T. J.; Grinter, R.; Thomson, A. J. *J. Chem. Soc.* **1978**, 608−611.

(11) Pratt, D. W.; Myers, R. J. *J. Am. Chem. Soc.* **1967**, *89*, 6470−6472.

(12) Rubinson, K. A.*J. Am. Chem. Soc.* **1976**, *98*, 5188−5191.

(13) Bratt, S. W.; Kassik, A.; Perutz, R. N.; Symons, M. C. R. *J. Am. Chem. Soc.* **1982**, *104*, 490−494.

(14) Ammeter, J. H.; Zoller, L.; Bachmann, J.; Baltzer, P.; Gamp, E.; Bucher, R.; Deiss, E. *Helv. Chim. Acta* **1981**, *64*, 1063−1082.

(15) Lever, A. B. P.; Ozin, G. A. *Inorg. Chem.* **1977**, *16*, 2012−2016.

(16) Huber, H.; Ford, T. A.; Klotzbücher, W.; Ozin, G. A. *J. Am. Chem. Soc.* **1976**, *98*, 3176−3178.

(17) DeKock, R. L. *Inorganic Chem.* **1971**, *10*, 1205−1211.

(18) Green, D. W.; Hodges, R. V.; Gruen, D. M. *Inorg. Chem.* **1976**, *15*, 970−972.

(19) Van Zee, R. J.; Ferrante, R. F.; Zeringue, K. J.; Weltner, W., Jr. *J. Chem. Phys.* **1988**, *88*, 3465−3474.

(20) Weltner, W., Jr. *Magnetic Atoms and Molecules*; Dover: New York, 1989.

(21) Stevens, K. W. H. *Proc. R. Soc. London Ser. A* **1953**, *219*, 542−555.

(22) Carrington, A.; McLachlan, A. D. *Introduction to Magnetic Resonance*; Harper and Row: New York, 1967.

(23) Dunn, T. M. *Trans Faraday Soc., London* **1961**, *57*, 1441−1444.

(24) Morton, J. R.; Preston, K. F. *J. Magn. Reson.* **1978**, *30*, 577−582.